A Microdosing Study with ^{99m}Tc-PHC-102 for the SPECT/CT Imaging of Primary and Metastatic Lesions in Renal Cell Carcinoma Patients

Oana C. Kulterer[1], Sarah Pfaff[1], Wolfgang Wadsak[1,2], Nathalie Garstka[3], Mesut Remzi[3], Chrysoula Vraka[1], Lukas Nics[1], Markus Mitterhauser[1,4], Franziska Bootz[5], Samuele Cazzamalli[5], Nikolaus Krall[6], Dario Neri[7], and Alexander R. Haug[1,8]

[1]Department of Biomedical Imaging and Image-Guided Therapy, Division of Nuclear Medicine, Medical University of Vienna, Vienna, Austria; [2]Center of Biomarker Research in Medicine, Graz, Austria; [3]Department of Urology, Medical University of Vienna, Vienna, Austria; [4]Ludwig Boltzmann Institute for Applied Diagnostics, Vienna, Austria; [5]Philochem AG, Otelfingen, Switzerland; [6]Allcyte GmbH, Vienna, Austria; [7]Department of Chemistry and Applied Biosciences, ETH Zürich, Zürich, Switzerland; and [8]Christian Doppler Laboratory for Applied Metabolomics, Medical University of Vienna, Vienna, Austria

^{99m}Tc-PHC-102 is a ^{99m}Tc-labeled derivative of acetazolamide, a high-affinity small organic ligand of carbonic anhydrase IX (CAIX). ^{99m}Tc-PHC-102 has previously shown favorable in vivo biodistribution properties in mouse models of CAIX-positive clear cell renal cell carcinoma (ccRCC) and colorectal cancer. In this study, we aimed to explore the targeting performance of ^{99m}Tc-PHC-102 in SPECT in patients with renal cell carcinoma while also assessing the safety and tolerability of the radiotracer. **Methods:** We studied 5 patients with localized or metastatic ccRCC in a microdosing regimen, after the administration of a 50-μg total of CAIX ligand and 600–800 MBq of ^{99m}Tc-PHC-102. Tissue distribution and residence time in normal organs and tumors were analyzed by serial SPECT/CT scans at 3 time points (30 min, 2 h, and 6 h) after intravenous administration. **Results:** In the 5 patients studied, ^{99m}Tc-PHC-102 was well tolerated and no study drug–related adverse events were recorded. In the stomach, kidneys, and gallbladder, the radiotracer showed a rapid initial uptake, which cleared over time. Localization of the study drug in primary tumors of 5 patients was observed, with favorable tumor-to-background ratios. ^{99m}Tc-PHC-102 SPECT/CT allowed the identification of 4 previously unknown lung and lymph node metastases in 2 patients. **Conclusion:** ^{99m}Tc-PHC-102 is a promising SPECT tracer for the imaging of patients with ccRCC. This tracer has the potential to identify primary and metastatic lesions in different anatomic locations. ^{99m}Tc-PHC-102 might also serve as a companion diagnostic agent for future CAIX-targeting therapeutics.

Key Words: clear cell renal cell carcinoma; carbonic anhydrase IX; SPECT; ^{99m}Tc; PHC-102

J Nucl Med 2021; 62:360–365
DOI: 10.2967/jnumed.120.245530

Carbonic anhydrase IX (CAIX) is a membrane-bound metalloenzyme involved in the maintenance of cellular acid–base homeostasis. CAIX is almost undetectable in normal adult-tissues, with the exception of certain organs of the gastrointestinal tract (*1–3*). This enzyme is nonetheless strongly expressed in most cases of clear cell renal cell carcinoma (ccRCC), as a result of von Hippel–Lindau mutations or deletions (*4*). Furthermore, at sites of hypoxia, a frequent condition in neoplastic solid masses, CAIX expression is abundant. Every year, more than 70,000 patients are diagnosed with kidney cancer in the United States, with a mortality rate of around 14,000 cases per year (www.cancer.gov). Most cases are CAIX-positive and, hence, provide an ideal target for imaging and drug delivery applications (*5*). In principle, CAIX ligands could be used to deliver radionuclides to the tumor site for imaging applications or for targeted radionuclide therapy (*6,7*). Moreover, CAIX ligands could be used for selective drug delivery applications, liberating cytotoxic agents at the tumor site and helping spare normal tissues (*7–12*).

The noninvasive detection of CAIX-positive tumors has been extensively studied using radiolabeled preparations of the cG250 antibody. In particular, ^{124}I-labeled cG250 could be used to localized ccRCC, with a satisfying tumor-to-kidney ratio of about 3:1 (*13*). Furthermore, the use of ^{124}I-cG250 immuno-PET/CT has shown a significantly higher detection rate of ccRCC than is possible with conventional CT (*14*). However, intact antibodies are not ideally suited for imaging applications, as their large size and slow clearance may lead to high radiation doses for patients (*13–15*). For this reason, it is desirable to target CAIX-positive tumors with radiolabeled preparations of small organic ligands, capitalizing on a better diffusion into the solid tumor mass and a faster clearance (*12,16*).

Initial attempts at targeting CAIX-positive tumors with radiolabeled aromatic sulfonamide derivatives had failed to show an acceptably high enrichment in neoplastic lesions, both in mouse models of cancer (*17,18*) and in patients (*19*). However, our group has previously shown that acetazolamide derivatives could be used for the selective delivery of radionuclides or fluorophores for imaging applications or therapy in CAIX-positive tumors (*6–8,11,12,20*). The use of charged linkers helped minimize ligand internalization into cells and, consequently, the undesired targeting of intracellular carbonic anhydrases (*8*).

^{99m}Tc-PHC-102 (^{99m}Tc-(3*S*)-3-{[(5*S*)-5-amino-5-{[(1*S*)-2-carboxy-1-{[(1*R*)-1-carboxy-2-sulfanylethyl]carbamoyl}ethyl]carbamoyl}pentyl]carbamoyl}-3-[5-(4-{3-[(5-sulfamoyl-1,3,4-thiadiazol-2-yl)carbamoyl]

Received Mar. 25, 2020; revision accepted Jun. 17, 2020.
For correspondence or reprints contact: Alexander R. Haug, Medical University of Vienna, Waehringer Gürtel 18-20, 1090 Vienna, Austria.
E-mail: alexander.haug@meduniwien.ac.at
Published online Jul. 17, 2020.

propyl}-1H-1,2,3-triazol-1-yl)pentanamido] propanoic acid) is a ^{99m}Tc-labeled acetazolamide derivative. Acetazolamide, an already-approved drug that is administered at doses of 0.5–1 g per patient (*21*), has shown promising biodistribution results in tumor-bearing mice (*6,7*). ^{99m}Tc is an attractive γ-emitting radionuclide for nuclear imaging applications, in view of its short half-life (6 h), easy production by generators (*22*), and good tolerability (*23,24*).

In this work, we aimed at assessing the safety and tolerability of ^{99m}Tc-PHC-102 while also exploring its tumor-targeting performance by SPECT imaging in patients with localized or metastatic ccRCC. We used a microdosing approach to capitalize on favorable regulatory guidelines for the execution of such studies in Europe and in the United States.

MATERIALS AND METHODS

Study Design and Patient Population

This first-in-humans prospective single-center, single-dose study was noncontrolled and nonrandomized and had an open-label, exploratory, microdosing design with a primary objective of assessing the safety and tolerability of ^{99m}Tc-PHC-102 in subjects with localized or metastatic ccRCC. As secondary objectives, the targeting performance in terms of biodistribution as fraction of injected activity, dosimetry (with a particular focus on tumor uptake), and pharmacokinetics was evaluated.

Five men 33–80 y old (mean ± SD, 62 ± 9.2) who had localized or metastatic ccRCC as confirmed by CT and optional histology and were scheduled for surgical resection of the primary renal mass were enrolled and imaged by SPECT/CT.

The study was authorized by the Austrian competent authority (AGES/BASG) and the Ethics Committee of the Medical University of Vienna. This trial was registered under EudraCT number 2016-004909-13 and was conducted in accordance with the Declaration of Helsinki, with the applicable regulatory requirements for Austria, according to International Conference on Harmonisation guidelines. All subjects provided written informed consent before participating in the study.

Radiopharmaceutical Preparation

^{99m}Tc-PHC-102 consists of the clinically approved carbonic anhydrase inhibitor acetazolamide moiety linked to a peptide-based ^{99m}Tc-chelator through a triazole-aspartic acid linker. ^{99m}Tc-PHC-102 was freshly prepared from the nonradioactive precursor (PHC-101) and sodium ^{99m}Tc-pertechnetate under reducing conditions for each patient and was immediately used for imaging purposes. Sodium ^{99m}Tc-pertechnetate was eluted from a commercially available and approved ^{99}Mo/^{99m}Tc-radionuclide generator (Mallinckrodt Pharmaceuticals) using sterile, isotonic saline solution as eluent. Unlabeled precursor PHC-101 (50 μg) was dissolved in degassed Tris-buffered saline buffer (pH 7.4). $SnCl_2$ (200 mg) and sodium glucoheptonate (20 mg) were added, followed by addition of sodium ^{99m}Tc-pertechnetate (generator eluate) in physiologic saline. The reaction mixture was heated to 95°C for 20 min and allowed to cool to room temperature. Subsequently, quality control was performed and pH, osmolality, and radiochemical and radionuclide purity were determined.

Dosage, Administration, and Dosimetry

The radiopharmaceutical ^{99m}Tc-PHC-102 was administered to the eligible patients under the supervision of the investigator intravenously as a single bolus injection in a volume of up to 10 mL through a peripheral venous catheter. Each dose consisted of a mean of 729 MBq (range, 608–797 MBq) of ^{99m}Tc-PHC-102 and a total of 50 μg of CAIX ligand (sum of radiolabeled ^{99m}Tc-PHC-102 and unlabeled PHC-101). Dosimetry was performed to precisely calculate the patient radiation burden from the radiopharmaceutical.

^{99m}Tc-PHC-102 SPECT/CT and Pharmacokinetics

Images were acquired using a SPECT/CT scanner (Symbia Intevo; Siemens Healthcare) at 30 min, 2 h, and 6 h after injection (a total of 3 scans per patient) using the xSPECT acquisition for quantitative SPECT. A low-dose CT scan (for attenuation correction and anatomic localization of the SPECT signal) preceded each scan. A whole-body SPECT acquisition covering the body from head to thighs was followed by the low-dose CT acquisition. SPECT data were normalized and corrected for attenuation, decay, and scatter. All scans were reconstructed and optimized to get the best image quality according to the specific uptake of the radiotracer.

Pharmacokinetics were determined by drawing blood (~1 mL) from a dedicated peripheral vein site into heparin-coated tubes. Blood was sampled at 5, 10, 30, and 60 min after administration, as well as at 2, 4, and 6 h. The volume of the samples (usually 1–1.5 mL) was determined by weighing the collection tubes before and after the blood sampling and assuming a blood density of 1.06 g/mL. The activity concentration in each sample was counted as MBq/mL using a γ-counter (Wizard^2; Perkin Elmer) and applied as a proxy of the tracer concentration in circulation. Blood activities were fit to a biphasic model, and α- and β-phase half-lives were reported for each patient.

Biodistribution and Image Analysis

The ^{99m}Tc-PHC-102 SPECT/CT images were assessed visually and quantitatively by evaluating the tumor and healthy-organ biodistribution and radiation dosimetry. Biodistribution was determined as the fraction of injected activity normalized to estimated organ or lesion weight as a function of time from administration for each lesion and healthy organ. Organ and lesion weights were estimated from volume, assuming a density of 1.0. Absorbed effective radiation doses were calculated according to the OLINDA methodology, using a software package (Hybrid Viewer 4.0 Dosimetry; Hermes Medical) for specific effective organ doses. Blood samples were used to assess bone marrow dosimetry. Lesion volumes were determined on the CT images acquired during the SPECT/CT scans. Volumes of interest were drawn manually around organs. A maximum tolerated total radiation burden was set at 10 mSv.

Safety Monitoring

For all participants, the safety of ^{99m}Tc-PHC-102 was evaluated on the basis of laboratory parameters (Supplemental Table 1; supplemental materials are available at http://jnm.snmjournals.org), vital signs, electrocardiograms, and physical examinations before and up to 6 h after intravenous administration of the radiotracer, and again during the follow-up visit (8 d after administration). Adverse events were continuously recorded.

Statistical Analysis

No statistical hypotheses were tested in the study, and the determination of the sample size is not applicable. Descriptive statistics were provided for dosimetry of lesions and healthy organs considering the specific absorbed dose (mSv/MBq) and the estimated dose (Gy), as well as pharmacokinetic parameters. The incidence for any adverse events was calculated considering severity and MedDRA (Medical Dictionary for Regulatory Activities) classification with system organ classes and preferred terms, together with vital signs, abnormal laboratory values, and physical examinations.

RESULTS

Radiolabeling Procedure

The procedure for incorporating ^{99m}Tc into the unlabeled precursor (PHC-101) was optimized to obtain radiochemical purity of at least 95% and specific activity of at least 23 MBq/μg. ^{99m}Tc-PHC-102 was freshly prepared before each injection (Supplemental

TABLE 1
Demographic Parameters and Histologic Information

Subject	Age (y)	Sex	Disease duration (y)	Histology–CAIX
1	80	M	<2	Positive
2	68	M	<2	Positive
3	80	M	<2	Positive
4	49	M	<2	Negative
5	32	M	<2	Unknown

Table 2). The dose was adjusted to 50 μg of CAIX ligand by dilution of the prepared ^{99m}Tc-PHC-102 dose (600–800 MBq) with a solution of PHC-101.

Disposition of Subjects and Safety Assessment

Five patients with ccRCC were enrolled in the study, which was conducted at the Department for Biomedical Imaging and Image-Guided Therapy, Division of Nuclear Medicine, Medical University in Vienna. The patients received the study drug and were imaged by SPECT/CT at multiple time points. Two patients with metastatic disease and 3 patients with primary renal cell carcinoma were enrolled. The characteristics of patients enrolled are shown in Table 1.

All 5 patients enrolled were evaluable for safety analysis. ^{99m}Tc-PHC-102 (a 50-μg total of CAIX ligand, 600–800 MBq) was well tolerated, and no clinically relevant adverse events were recorded. Hematologic parameters were also not affected (Supplemental Table 1).

Biodistribution and Pharmacokinetics of ^{99m}Tc-PHC-102

A dosimetric analysis revealed an overall effective dose per patient of 6.3 ± 1.7 mSv (Supplemental Table 3). The organ-specific SUV_{max} and SUV_{mean} at 30 min, 2 h, and 6 h after injection are shown in Table 2.

A pharmacokinetic analysis (Fig. 1), based on radioactive counting of blood specimens at multiple time points revealed a biphasic clearance profile with a fast half-time of 0.1361 h, corresponding to 55.0% of the clearance profile, and a slow half-time of 1.35, corresponding to the remaining 44.9% of the clearance profile (*25*).

Imaging Results

Patient 1 (an 80-y-old man) had been diagnosed with CAIX-positive ccRCC after experiencing abdominal discomfort and hematuria for several months. At the time of the diagnosis, the patient already had lymph node metastasis. A 7.2-cm lesion in the left kidney was clearly visible 6 h after injection of ^{99m}Tc-PHC-102 in both whole-body planar and transverse ^{99m}Tc-PHC-102 SPECT/CT scans (Figs. 2A and 2B). Radiotracer uptake in the stomach and gallbladder was also observed, in line with published CAIX expression patterns. Surprisingly, a previously unknown pulmonary metastatic lesion of 2.3 cm in the right upper lobe was also detected at all imaging time points (0.5, 2, and 6 h) (Fig. 2C).

Patient 2 (a 68-y-old man) was admitted to the hospital because of perforated appendicitis. A native CT scan showed a 2.5-cm lesion in the upper kidney pole. A later MRI exam with arterial enhancement showed a suspected renal cell carcinoma lesion, which was confirmed on biopsy. CAIX was positive only in isolated cells. In the ^{99m}Tc-PHC-102 SPECT/CT scan, the lesion protruding from the cortex of the right kidney was detectable at all time points (Fig. 3).

Patient 3 (an 80-y-old man) already had a diagnosis of ccRCC with lymph nodes metastases. The ^{99m}Tc-PHC-102 SPECT/CT scan showed physiologic uptake in the stomach and gut. Moreover, there was an inhomogeneous tracer accumulation in the right renal bed, assignable to the extended tumor mass. At the admission time point, a tumor mass was detectable in the vena cava. ^{99m}Tc-PHC-102 uptake inferiorly in the vena cava corresponded to the intravenous tumor mass. Interestingly, focal ^{99m}Tc-PHC-102 uptake was observed in the left upper lung lobe but was not previously described in CT reports (Fig. 4).

TABLE 2
^{99m}Tc-PHC-102 SUVs Corresponding to Different Time Points

	SUV_{max}			SUV_{mean}		
Organ	30 min	2 h	6 h	30 min	2 h	6 h
Tumor	20.14 ± 3.94	18.43 ± 5.15	15.48 ± 4.74	14.02 ± 3.32	11.7 ± 3.08	10.38 ± 2.07
Kidney	35.04 ± 6.50	26.6 ± 4.05	17.50 ± 2.19	19.68 ± 4.49	16.75 ± 1.75	12.24 ± 1.33
Liver	4.26 ± 1.13	5.43 ± 1.11	6.06 ± 3.08	3.1 ± 1.16	4.00 ± 1.14	4.54 ± 2.57
Gallbladder	9.23 ± 3.66	17.2 ± 6.58	28.58 ± 11.80	6.55 ± 2.48	10.65 ± 2.77	15.28 ± 3.99
Intestine	6.78 ± 1.03	11.3 ± 4.57	10.80 ± 3.39	3.44 ± 1.12	3.65 ± 0.60	3.04 ± 0.93
Lung	0.94 ± 0.32	0.85 ± 0.30	0.56 ± 0.26	0.58 ± 0.26	0.40 ± 0.27	0.22 ± 0.13
Brain	0.32 ± 0.15	0.375 ± 0.22	0.28 ± 0.17	0.12 ± 0.12	0.11 ± 0.13	0.06 ± 0.05
Stomach	47.68 ± 15.63	58.5 ± 16.42	49.18 ± 28.54	21.22 ± 5.93	24.88 ± 6.12	20.96 ± 8.14
Spleen	1.28 ± 0.29	0.925 ± 0.34	0.78 ± 0.13	0.62 ± 0.26	0.35 ± 0.21	0.22 ± 0.08
Salivary gland	3.02 ± 2.52	1.32 ± 2.38	1.60 ± 0.94	2.3 ± 1.69	1.83 ± 1.31	1.08 ± 0.64

Average SUV_{max} and SUV_{mean} are based on individual values from 5 patients imaged with microdosing ^{99m}Tc-PHC-102 SPECT/CT.

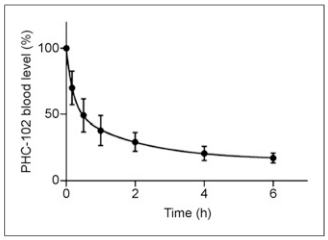

FIGURE 1. ^{99m}Tc-PHC-102 blood levels. Blood clearance profiles were assessed by collecting blood samples at different time points and counting corresponding radioactivity values. Curve was calculated as average of values derived from individual patients. Variations in clearance rate were observed, possibly reflecting differences in kidney function.

Patient 4 (a 49-y-old man) presented with hematuria at a routine check-up. Kidney ultrasound revealed a 1.9-cm kidney lesion in the hilum. Biopsy results showed CAIX-positive ccRCC. The ^{99m}Tc-PHC-102 SPECT/CT scan revealed a hilum lesion with low tracer uptake at all imaging time points.

Patient 5 (a 32-y-old man) was in treatment at a fertility clinic. A routine urine examination showed microhematuria. A CT examination showed a 3.5-cm lesion in the lower left kidney pole, which turned out to be ccRCC on histologic examination. The ^{99m}Tc-PHC-102 SPECT/CT scan revealed weak tracer accumulation at all imaging time points.

DISCUSSION

This study showed that ccRCC patients can safely be imaged using ^{99m}Tc-PHC-102 SPECT/CT. The methodology is easy to implement in routine clinical practice and provides valuable information such as uptake in primary lesions and detection of previously unknown metastatic lesions.

CAIX is physiologically expressed in the stomach, small intestine, and gallbladder. Small molecules reach those structures in vivo more efficiently than antibodies do, reflecting a higher extravasation rate and easier diffusion into tissues (*13*). We have previously reported that stomach and kidney uptake decreases at higher doses of PHC-102, with a possible benefit for both imaging and therapy applications (*6*). The uptake quantification reported in this first microdosing study compares well with that reported for other successful radiopharmaceuticals (e.g., PSMA ligands) (*26*). Thus, it is possible that PHC-102 analogs, labeled with an α- or β-emitting radionuclide, may be suitable for radionuclide therapy.

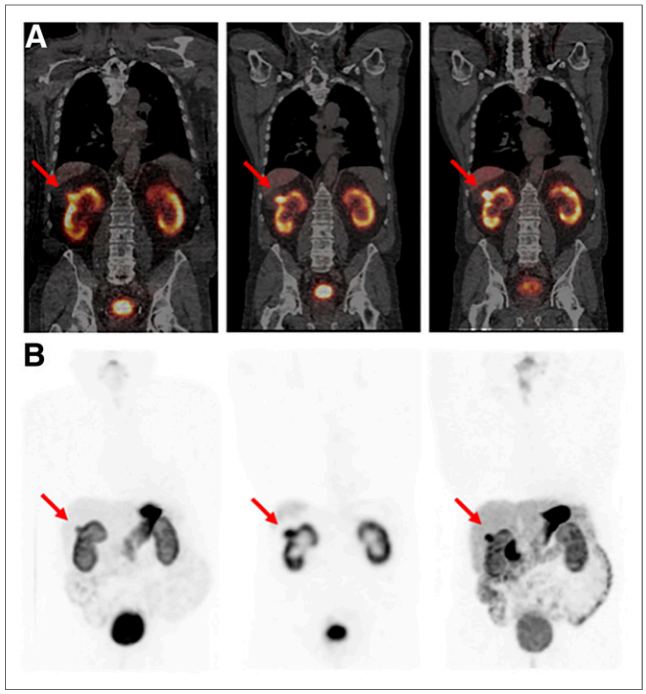

FIGURE 3. Anterior SPECT/CT (A) and SPECT (B) scans obtained with ^{99m}Tc-PHC-102 in 49-y-old patient at (from left to right) 30 min, 2 h, and 6 h after administration of tracer. Primary neoplastic lesion (arrows) protruding from cortex of right kidney (1.6 cm) is visible at all time points. Renal excretion is appreciable from high signal observed in bladder at 30-min time point and from kidney uptake.

The detection of metastatic lesions has particular medical value in ccRCC patients. Although early-stage disease with localized tumors typically undergoes surgical intervention (*27*), systemic administration of VEGFR inhibitors, TKIs, and anti-PD-1 and anti-PD-L1 antibodies represents the preferred treatment option for metastatic ccRCC (*28*). In the imaging of metastatic lesions, it would be interesting to perform a side-by-side comparison

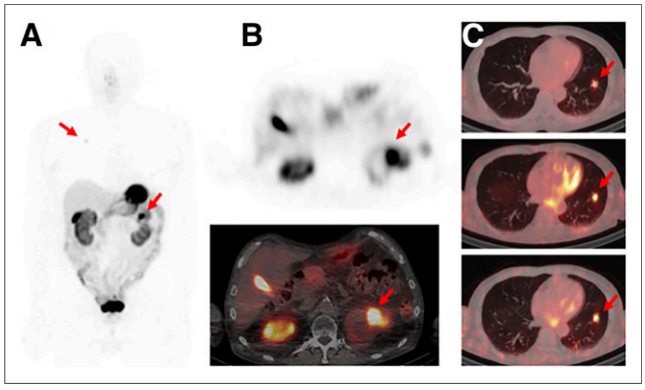

FIGURE 2. Anterior whole-body planar (A) and transverse SPECT (B) and ^{99m}Tc-PHC-102 fused SPECT/CT (C) images in 80-y-old patient with ccRCC (CAIX-positive). High uptake of radiotracer (arrows) in primary tumor (7.2 cm, upper pole of left kidney), in stomach, and in gallbladder was observed. Additional metastatic lesion (2.3 × 1.6 cm) in lung was also detected at all time points (0.5, 2, and 6 h).

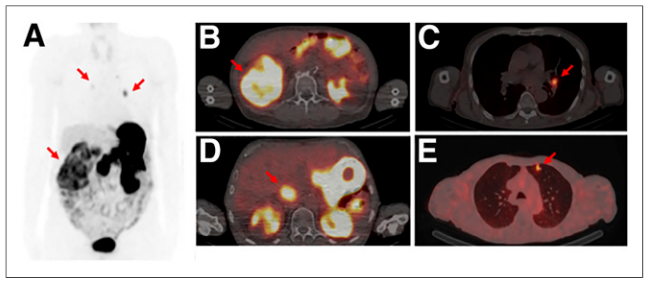

FIGURE 4. Anterior SPECT (arrows indicate RCC and metastases) (A) and transverse SPECT/CT (B) scans obtained with ^{99m}Tc-PHC-102 in 80-y-old patient at 6-h time point. Primary large tumor mass (A and B) in right kidney (7.2 cm, arrow in B indicates RCC) was detectable because of high tracer uptake. Tumor thrombus in vena cava (B and C; indicated with an arrow in C), as well as metastatic lesions in lymph node (D, indicated with an arrow) and in lung (E, indicated with an arrow), were also visible 6 h after ^{99m}Tc-PHC-102 injection because of high tracer uptake.

between ^{99m}Tc-PHC-102 and conventional radiotracers (e.g., ^{18}F-FDG, as application of ^{18}F-FDG PET/CT showed limitations for ccRCC detection due to the physiologic excretion of ^{18}F-FDG through the kidneys, which decreases contrast between healthy tissue and neoplastic lesions (*29–31*).

Our results suggest that CAIX lesions can efficiently be targeted with acetazolamide derivates in patients with localized or metastatic ccRCC. We have previously shown that acetazolamide-based small-molecule drug conjugates target CAIX-positive tumors more efficiently than does their antibody-drug conjugate (ADC) counterpart (*12*). Indeed, small-molecule drug conjugate products may be ideally suited for the selective delivery of potent cytotoxic agents such as monomethylauristatin E (*10,12*). Small-molecule drug conjugates synergize with tumor-targeting antibody-interleukin-2 fusions (*11*). Recombinant human interleukin-2 is approved for the treatment of metastatic renal cell carcinoma (*32,33*), and it appears that the antibody-based delivery of this cytokine to the tumor side may potentiate activity while helping spare normal tissues (*34–36*). In this context,^{99m}Tc- PHC-102 may represent a useful companion diagnostic for the clinical development of CAIX-specific small-molecule drug conjugates, in full analogy to what was previously implemented by scientists at Endocyte for the molecular targeting of folate receptor (*37–39*) and of PSMA (*40,41*).

CONCLUSION

Our data show that ^{99m}Tc-PHC-102 appears to be well suited for the molecular imaging of CAIX-positive ccRCC. SPECT/CT procedures reveal anatomic localization of primary and metastatic lesions and may be easier to implement than PET analysis, in terms of scanner accessibility and ease of radioactive labeling. The possibility of imaging patients a few hours after intravenous administration of the radiotracer should facilitate the routine implementation of ^{99m}Tc-PHC-102 methodologies, as compared with similar procedures based on monoclonal antibodies, which also gave excellent imaging results but at later time points and with a higher radiation burden for the patients. The successful imaging of ccRCC lesions (including previously unknown metastatic masses) provides a motivation to continue studying the tumor-targeting properties of ^{99m}Tc-PHC-102 at higher doses and in a variety of different CAIX-positive tumors (e.g., colorectal and urothelial cancer). Future studies will show whether ^{99m}Tc-PHC-102 can also detect antigen-positive lesions in other tumor types (e.g., colorectal cancer, urothelial cancer, and high-grade astrocytomas) known to express CAIX (*42*).

DISCLOSURE

This project received funding from the European Community (grant E!9669 ATRI), the Swiss National Science Foundation (grant 310030_182003/1), and the European Research Council (ERC) under the European Union's Horizon 2020 research and innovation program (grant agreement 670603). Dario Neri was supported by ETH Zurich and is a cofounder and shareholder of Philogen S.p.A. (www.philogen.com), a Swiss-Italian Biotech company that owns PHC-102. Samuele Cazzamalli is an employee of Philochem AG. Nikolaus Krall is entitled to shares of licensing revenues from ETH for PHC-102. No other potential conflict of interest relevant to this article was reported.

KEY POINTS

QUESTION: Can ^{99m}Tc-PHC-102, a novel CAIX-targeted radiotracer, be used for diagnostic purposes to detect primary tumors and metastatic lesions in patients with renal cell carcinoma?

PERTINENT FINDINGS: Our microdosing results in 5 renal cell carcinoma patients confirmed that ^{99m}Tc-PHC-102 localizes in primary tumors, with favorable tumor-to-background ratios. ^{99m}Tc-PHC-102 SPECT/CT allowed the identification of previously unknown lung and lymph node metastases in 2 patients.

IMPLICATIONS FOR PATIENT CARE: ^{99m}Tc-PHC-102 is a promising SPECT tracer for the imaging of patients with ccRCC, with the potential to identify primary and metastatic lesions in different anatomic locations.

REFERENCES

1. Supuran CT. Inhibition of carbonic anhydrase IX as a novel anticancer mechanism. *World J Clin Oncol.* 2012;3:98–103.
2. Takacova M, Bartosova M, Skvarkova L, et al. Carbonic anhydrase IX is a clinically significant tissue and serum biomarker associated with renal cell carcinoma. *Oncol Lett.* 2013;5:191–197.
3. Uhlén M, Bjorling E, Agaton C, et al. A human protein atlas for normal and cancer tissues based on antibody proteomics. *Mol Cell Proteomics.* 2005;4:1920–1932.
4. Bui MH, Seligson D, Han KR, et al. Carbonic anhydrase IX is an independent predictor of survival in advanced renal clear cell carcinoma: implications for prognosis and therapy. *Clin Cancer Res.* 2003;9:802–811.
5. Wang Y, Wang XY, Subjeck JR, Kim HL. Carbonic anhydrase IX has chaperone-like functions and is an immunoadjuvant. *Mol Cancer Ther.* 2008;7:3867–3877.
6. Krall N, Pretto F, Mattarella M, Muller C, Neri D. A technetium 99m-labeled ligand of carbonic anhydrase IX selectively targets renal cell carcinoma in vivo. *J Nucl Med.* 2016;57:943–949.
7. Cazzamalli S, Dal Corso A, Neri D. Acetazolamide serves as selective delivery vehicle for dipeptide-linked drugs to renal cell carcinoma. *Mol Cancer Ther.* 2016; 15:2926–2935.
8. Krall N, Pretto F, Decurtins W, Bernardes GJ, Supuran CT, Neri D. A small-molecule drug conjugate for the treatment of carbonic anhydrase IX expressing tumors. *Angew Chem Int Ed Engl.* 2014;53:4231–4235.
9. Krall N, Pretto F, Neri D. A bivalent small molecule-drug conjugate directed against carbonic anhydrase IX can elicit complete tumour regression in mice. *Chem Sci.* 2014;5:3640–3644.
10. Cazzamalli S, Corso AD, Neri D. Linker stability influences the anti-tumor activity of acetazolamide-drug conjugates for the therapy of renal cell carcinoma. *J Control Release.* 2017;246:39–45.
11. Cazzamalli S, Ziffels B, Widmayer F, et al. Enhanced therapeutic activity of non-internalizing small-molecule-drug conjugates targeting carbonic anhydrase IX in combination with targeted interleukin-2. *Clin Cancer Res.* 2018;24:3656–3667.
12. Cazzamalli S, Dal Corso A, Widmayer F, Neri D. Chemically defined antibody- and small molecule-drug conjugates for in vivo tumor targeting applications: a comparative analysis. *J Am Chem Soc.* 2018;140:1617–1621.
13. Divgi CR, Pandit-Taskar N, Jungbluth AA, et al. Preoperative characterisation of clear-cell renal carcinoma using iodine-124-labelled antibody chimeric G250 (^{124}I-cG250) and PET in patients with renal masses: a phase I trial. *Lancet Oncol.* 2007;8:304–310.
14. Divgi CR, Uzzo RG, Gatsonis C, et al. Positron emission tomography/computed tomography identification of clear cell renal cell carcinoma: results from the REDECT trial. *J Clin Oncol.* 2013;31:187–194.
15. Dennis MS, Jin H, Dugger D, et al. Imaging tumors with an albumin-binding Fab, a novel tumor-targeting agent. *Cancer Res.* 2007;67:254–261.
16. Yuan F, Dellian M, Fukumura D, et al. Vascular permeability in a human tumor xenograft: molecular size dependence and cutoff size. *Cancer Res.* 1995;55: 3752–3756.
17. Peeters SG, Dubois L, Lieuwes NG, et al. [^{18}F]VM4-037 microPET imaging and biodistribution of two in vivo CAIX-expressing tumor models. *Mol Imaging Biol.* 2015;17:615–619.
18. Dubois L, Lieuwes NG, Maresca A, et al. Imaging of CA IX with fluorescent labelled sulfonamides distinguishes hypoxic and (re)-oxygenated cells in a xenograft tumour model. *Radiother Oncol.* 2009;92:423–428.

19. Doss M, Kolb HC, Walsh JC, et al. Biodistribution and radiation dosimetry of the carbonic anhydrase IX imaging agent [^{18}F]VM4-037 determined from PET/CT scans in healthy volunteers. *Mol Imaging Biol.* 2014;16:739–746.
20. Wichert M, Krall N, Decurtins W, et al. Dual-display of small molecules enables the discovery of ligand pairs and facilitates affinity maturation. *Nat Chem.* 2015;7:241–249.
21. Low EV, Avery AJ, Gupta V, Schedlbauer A, Grocott MP. Identifying the lowest effective dose of acetazolamide for the prophylaxis of acute mountain sickness: systematic review and meta-analysis. *BMJ.* 2012;345:e6779.
22. Liu S, Edwards DS, Barrett JA. ^{99m}Tc labeling of highly potent small peptides. *Bioconjug Chem.* 1997;8:621–636.
23. Fisher RE, Siegel BA, Edell SL, et al. Exploratory study of ^{99m}Tc-EC20 imaging for identifying patients with folate receptor-positive solid tumors. *J Nucl Med.* 2008;49:899–906.
24. Barrett JA, Coleman RE, Goldsmith SJ, et al. First-in-man evaluation of 2 high-affinity PSMA-avid small molecules for imaging prostate cancer. *J Nucl Med.* 2013;54:380–387.
25. Borsi L, Balza E, Bestagno M, et al. Selective targeting of tumoral vasculature: comparison of different formats of an antibody (L19) to the ED-B domain of fibronectin. *Int J Cancer.* 2002;102:75–85.
26. Afshar-Oromieh A, Malcher A, Eder M, et al. PET imaging with a [^{68}Ga]gallium-labelled PSMA ligand for the diagnosis of prostate cancer: biodistribution in humans and first evaluation of tumour lesions. *Eur J Nucl Med Mol Imaging.* 2013;40:486–495.
27. Escudier B, Porta C, Schmidinger M, et al. Renal cell carcinoma: ESMO clinical practice guidelines for diagnosis, treatment and follow-up. *Ann Oncol.* 2016;27:v58–v68.
28. Rodriguez-Vida A, Hutson TE, Bellmunt J, Strijbos MH. New treatment options for metastatic renal cell carcinoma. *ESMO Open.* 2017;2:e000185.
29. Wang HY, Ding HJ, Chen JH, et al. Meta-analysis of the diagnostic performance of [^{18}F]FDG-PET and PET/CT in renal cell carcinoma. *Cancer Imaging.* 2012;12:464–474.
30. Aide N, Cappele O, Bottet P, et al. Efficiency of [^{18}F]FDG PET in characterising renal cancer and detecting distant metastases: a comparison with CT. *Eur J Nucl Med Mol Imaging.* 2003;30:1236–1245.
31. Miyakita H, Tokunaga M, Onda H, et al. Significance of ^{18}F-fluorodeoxyglucose positron emission tomography (FDG-PET) for detection of renal cell carcinoma and immunohistochemical glucose transporter 1 (GLUT-1) expression in the cancer. *Int J Urol.* 2002;9:15–18.
32. Amin A, White RL. Interleukin-2 in renal cell carcinoma: a has-been or a still-viable option? *J Kidney Cancer VHL.* 2014;1:74–83.
33. Rosenberg SA, Yang JC, Topalian SL, et al. Treatment of 283 consecutive patients with metastatic melanoma or renal cell cancer using high-dose bolus interleukin 2. *JAMA.* 1994;271:907–913.
34. Carnemolla B, Borsi L, Balza E, et al. Enhancement of the antitumor properties of interleukin-2 by its targeted delivery to the tumor blood vessel extracellular matrix. *Blood.* 2002;99:1659–1665.
35. Johannsen M, Spitaleri G, Curigliano G, et al. The tumour-targeting human L19-IL2 immunocytokine: preclinical safety studies, phase I clinical trial in patients with solid tumours and expansion into patients with advanced renal cell carcinoma. *Eur J Cancer.* 2010;46:2926–2935.
36. Eigentler TK, Weide B, de Braud F, et al. A dose-escalation and signal-generating study of the immunocytokine L19-IL2 in combination with dacarbazine for the therapy of patients with metastatic melanoma. *Clin Cancer Res.* 2011;17:7732–7742.
37. Leamon CP, Parker MA, Vlahov IR, et al. Synthesis and biological evaluation of EC20: a new folate-derived, ^{99m}Tc-based radiopharmaceutical. *Bioconjug Chem.* 2002;13:1200–1210.
38. Pribble P, Edelman MJ. EC145: a novel targeted agent for adenocarcinoma of the lung. *Expert Opin Investig Drugs.* 2012;21:755–761.
39. Naumann RW, Coleman RL, Burger RA, et al. PRECEDENT: a randomized phase II trial comparing vintafolide (EC145) and pegylated liposomal doxorubicin (PLD) in combination versus PLD alone in patients with platinum-resistant ovarian cancer. *J Clin Oncol.* 2013;31:4400–4406.
40. Wang J, Zang J, Wang H, et al. Pretherapeutic ^{68}Ga-PSMA-617 PET may indicate the dosimetry of ^{177}Lu-PSMA-617 and ^{177}Lu-EB-PSMA-617 in main organs and tumor lesions. *Clin Nucl Med.* 2019;44:431–438.
41. Rathke H, Giesel FL, Flechsig P, et al. Repeated ^{177}Lu-labeled PSMA-617 radioligand therapy using treatment activities of up to 9.3 GBq. *J Nucl Med.* 2018;59:459–465.
42. Wykoff CC, Beasley NJ, Watson PH, et al. Hypoxia-inducible expression of tumor-associated carbonic anhydrases. *Cancer Res.* 2000;60:7075–7083.